NISTIR 88-3873

# Small Angle X-Ray Study of the Deformation of 4,4′-Diphenylmethane Diisocyanate/1,4′-Butanediol (MDI/BDO) Based Polyurethanes

R. M. Briber, P. Sung and J. D. Barnes

U.S. DEPARTMENT OF COMMERCE
National Institute of Standards and Technology
(Formerly National Bureau of Standards)
Institute for Materials Science and Engineering
Polymers Division
Polymer Blends Group
Gaithersburg, MD 20899

October 1988

NISTIR 88-3873

# Small Angle X-Ray Study of the Deformation of 4,4′-Diphenylmethane Diisocyanate/1,4′-Butanediol (MDI/BDO) Based Polyurethanes

R. M. Briber, P. Sung and J. D. Barnes

U.S. DEPARTMENT OF COMMERCE
National Institute of Standards and Technology
(Formerly National Bureau of Standards)
Institute for Materials Science and Engineering
Polymers Division
Polymer Blends Group
Gaithersburg, MD 20899

October 1988

National Bureau of Standards became the National Institute of Standards and Technology on August 23, 1988, when the Omnibus Trade and Competitiveness Act was signed. NIST retains all NBS functions. Its new programs will encourage improved use of technology by U.S. industry.

**U.S. DEPARTMENT OF COMMERCE**
**C. William Verity, Secretary**

**NATIONAL INSTITUTE OF STANDARDS AND TECHNOLOGY**
**Ernest Ambler, Director**

ABSTRACT

Small angle x-ray scattering (SAXS) has been used to study the effect of deformation on the hard segment domain morphology of a series of segmented polyurethanes based on 4,4'-diphenylmethane diisocyanate/1,4'-butanediol (MDI/BDO) as the hard segment and polytetramethylene oxide (PTMO) as the soft segment. At relatively low elongations (100-200%) the hard segment lamellae orient and align with their long axis perpendicular to the deformation direction. As the deformation increases (200-400%) these aligned domains begin to break down and the SAXS intensity decreases correspondingly. At the largest deformations (400-500%) a new component to the scattering appears as a streak running perpendicular to the deformation direction and subsequent optical microscopy reveals the presence of crazes. Crazes have been observed at elongations close to failure in all three polyurethanes studied so far, yet the presence of crazing has not been recognized in the scientific literature as being important in understanding the deformation behavior of polyurethanes.

## INTRODUCTION

Polyurethanes are segmented copolymers where the two different blocks on the polymer chain are thermodynamically incompatible in the normal range of use temperatures. This leads to microphase separation of the two blocks (hard and soft segments) and at compositions of ~50% hard segment and less, hard segment microdomains on the order of 10 nm in size are formed which act as reinforcing physical crosslinks for the soft segment matrix. These hard segment domains give polyurethanes their desirable properties of high toughness and the ability to tailor the properties to meet specific end uses by varying the ratio of hard and soft segment [1].

Polyurethanes based on 4,4′ diphenylmethane diisocyanate (MDI) and 1,4-butanediol (BDO) as the hard segment (henceforth termed MDI/BDO) combined with various soft segments are very important commercially [1]. In this work we will study the system consisting of MDI/BDO as the hard segment and polytetramethylene oxide (PTMO, prepolymer molecular weight $M_n$=1000) as the soft segment. The focus of the work presented here will be the changes that occur in the hard segment domain morphology with deformation as studied by small angle x-ray scattering (SAXS). The morphology of MDI/BDO based polyurethanes in the isotropic state has been the subject of numerous articles in the literature [2-8] but the behavior with deformation has not been studied with the same depth.

## BACKGROUND

MDI/BDO hard segments have been shown to form two distinct crystal

structures in the isotropic state (type I and type II) and a third crystal structure is found on deformation (type III) [9]. Previous work has shown that the type II crystal structure (the more highly ordered of the two structures which appear in the isotropic state) forms lamellar hard segment domains about 12nm in width by about 50-70nm in length for high hard segment content materials [10], with smaller lamellae being formed for lower hard segment content materials. A wide angle x-ray scattering (WAXS) deformation study on the same type of materials as studied in this paper has shown that, at least at the higher hard segment contents, (46 wt%) there is a continuous shift in the hard segment chain axis WAXS reflection to smaller angles with increasing deformation. This indicates that the hard segment chain conformation is changing continuously with deformation [11]. The length of the hard segment repeat unit increases with deformation, shifting towards the chain conformation characteristic of the type III crystal structure. At large elongations (500%), there remains extensive disorder between neighboring chains along the deformation direction and the type III structure is not obtained without subsequent annealing in the deformed state.

Small angle x-ray scattering of polyurethanes has been studied by numerous authors [1,7,8,12-17] but only a relatively small number of these were concerned with morphology changes that occurred with deformation [15-17]. In general it has been observed by both infrared dichroism and WAXS at low elongations (<100%) in polyurethanes the hard segment chains initially orient perpendicular to the deformation and subsequently at larger deformations (>100%), orient parallel to the deformation direction [18-20]. In this work only the deformation behavior at strains greater than 100% will be considered in detail.

## EXPERIMENTAL

The polyurethanes were supplied in the form of melt pressed sheets 15 cm square and 0.12 cm thick by the Upjohn Corporation under the trade name Pellethane [21]. The polyurethanes are based on MDI/BDO as the hard segment and PTMO ($M_n$=1000) as the soft segment. Three samples of different hard segment content termed Pellethane 80A, 90A and 55D (increasing hard segment content) were studied and the molar ratios, average hard segment length (assuming a most probable sequence length distribution [22-24]) and weight percent hard segment are given in table 1. All samples were annealed at 140°C for 12 hours before any mechanical testing or SAXS experiments were performed in order to provide an equivalent and reproducible thermal treatment and morphology for the samples. Mechanical testing was performed using a Tinius-Olsen testing machine [21]. The strain rate for all deformation experiments was 10 cm/min. To prepare the samples for SAXS the specimens were stretched to the desired elongation and then clamped using a pair of steel plates with a 2cm by 1cm hole machined in the center. Gauge marks drawn with a pen on the samples were used to measure the strain and to assure that the clamping procedure did not result in significant change in the deformation. SAXS was performed using the NBS 10 meter digital SAXS camera. This camera utilizes a 12 kW Rigaku-Denki rotating anode x-ray generator producing Cu $K_\alpha$ ($\lambda$=1.5418) radiation which was passed through a graphite monochromator [21]. The data was collected using a two dimensional position sensitive gas filled detector manufactured by TEC [21]. The data was corrected for parasitic scattering,

sample thickness and transmission, normalized to a constant monitor count and then put on a absolute scale using a secondary standard which had been calibrated against a Lupolen standard. The data was then circularly averaged in the case of the isotropic samples and sector averaged (25° sector width) parallel and perpendicular to the deformation direction for the deformed samples.

## RESULTS AND DISCUSSION

Figure 1 shows the typical stress strain curves for the 80A, 90A and 55D samples (circles, squares and triangles respectively). SAXS patterns were taken at elongations of 0%, 100%, 200%, 300% (80A, 55D), 350% (90A), 400% (80A, 55D), 450% (90A, 55D) and 500% (80A). The figures 2a-f, 3a-e and 4a-f are the two dimensional SAXS patterns from the three polyurethanes at the different levels of deformation. The intensity scale is mapped onto a false color scheme with the scale shown at the edge of each of the figures. With increasing intensity the colors change in the order black-red-yellow-white-green-blue-purple. A clear peak in the scattering pattern is observed for all three samples at 0% deformation (2a, 3a, and 4a). The circularly averaged data for the 0% deformation samples was Lorentz corrected by multiplying the intensity data by $q^2$ (q is the scattering vector given by $q=4\pi\sin\theta/\lambda$) as is normally done for lamellar systems [25]. This data for the three isotropic samples is shown in figure 5. The positions of the peak and the equivalent lamellar spacings, d, calculated using Bragg's law ($d=\lambda/2\sin\theta$), are given in table 3.

The two dimensional patterns for the samples stretched to 100% and 200% elongation are given in figures 2b,c 3b,c and 4b,c respectively. The

deformation direction is shown by the arrow. The patterns show an clear evidence of the deformation with maximum due to the lamellar periodicity orienting along the meridian. The scattered intensity is also diminished in the equatorial region of the pattern. This indicates an alignment of the hard lamellae with their long axis perpendicular to the deformation direction and consequently the hard segment chain axis is oriented along the deformation direction.

Figures 2d, 3d and 4d show the two dimensional SAXS data obtained at 300% elongation for samples 80A and 55D and 350% for the 90A sample. Figures 2e, 3e and 4e show the data for the 80A, 90A and 55D samples at 400%, 450% and 400% deformation respectively. Figures 2f and 4f show the data at 500% and 450% for the 80A and 55D samples.

The first obvious trend observable in the data is that as the deformation starts (100%) all the samples exhibit orientation of the hard segment lamellae along the direction perpendicular to the deformation. At slightly higher elongations (200%) the orientation of the domains is increased, but at the same time it becomes apparent, especially in the 55D sample that the scattered intensity is decreasing. Figures 6a,b 7a,b and 8a,b show I(q) versus q plots along the equator and meridian for the data presented in the two dimensional scattering patterns for the 80A, 90A and 55D samples respectively. The data presented in figures 6-8 was averaged over 25° wide sectors perpendicular (equatorial) and parallel (meridian) to the deformation direction. The decreasing intensity with deformation is clearly visible in the I(q) versus q plots where the scattering maximum decreases continuously with deformation both along the equator and the meridian.

In the two dimensional patterns there is an additional effect that is

observable at the larger deformations. There is a pronounced streaking in the equatorial regions of the scattering pattern clearly visible in figures 2d, 3d and 4d, though it is beginning to show up at 200% deformation (figures 2c, 3c, and 4c). This streaking appears to start earlier for the higher hard segment content 55D sample but becomes the most pronounced for the 80A sample at 500% deformation. The 80A sample deformed to 500% exhibits a large increase in the equatorial scattering at the smallest angles which is clearly visible as a region of purple in figure 2f. The increased scattering is also present in the equatorial sector average in figure 6a where the scattering at 500% deformation is much larger in the q region between 0.01-0.04 $Å^{-1}$. One possible explanation for the increased scattering is void formation at the largest deformations and indeed the 90A and 55D samples begin to scatter light, becoming slightly hazy, shortly before failure (~350%). The 80A sample begins whitening at about 450%, eventually becoming opaque at failure. Closer examination of an 80A sample at large deformations by optical microscopy reveals that the source of the stress whitening is crazing. Figures 9a and b are optical micrographs taken using dark field and phase contrast optics of an 80A sample stretched to 500% and 700% deformation respectively. An arrow on each micrograph indicates the deformation direction. Figure 9a is at lower magnification and the crazing is seen as lines running perpendicular to the deformation direction. In figure 9b at higher magnification the larger deformation has caused the crazes to open up and the internal structure can be seen to consist of fibrils running perpendicular to the craze boundaries (parallel to the deformation direction). Optical microscopy on the 90A and 55D samples also reveals the presence of crazes at large deformations, with the number density of crazes appearing to decrease with increasing hard segment content at constant elongation. Crazing

has been reported in polyurethanes only once before [26] and the presence of crazes prior to failure is not widely appreciated. The streaking the SAXS patterns observed along the equator is probably due to elliptical voids (with the major axis oriented along the deformation direction) occurring between the fibrils inside the crazes rather than due to scattering from periodicity between the separate crazes (which is on the order of tens of microns and would be at too small an angle to resolve by SAXS). At the large deformations attained shortly before failure the hard segment domain structure is essentially completely destroyed and the scattering from the crazes dominates the SAXS patterns.

## CONCLUSIONS

From the work currently being completed it has been shown that the domain morphology first orients with the hard segment lamellae perpendicular to the draw direction and then, with increasing deformation, the domains begin to break down. As the sample approaches the elongation at fracture, $\epsilon_f$, the hard segment domains are completely destroyed and the material begins to exhibit crazing. At slightly larger deformations the polyurethane fails. This behavior is present in all the polyurethanes studied so far including Pellethane 80A, 90A and 55D. It is not known whether the morphology of the hard segment domains will return to the same (or similar) state upon releasing of the strain (at strain levels less then $\epsilon_f$) after it has been held in the stretched state for a period of time.

## EXTENSIONS AND FUTURE WORK

Experiments are planned to extend the current work to study the recovery

of the polyurethanes after uniaxial stretching. Small angle x-ray scattering will again be used to study the domain morphology both before and after the releasing of the strain. This work should give valuable insight into the deformation processes that occur in polyurethanes under cyclic deformation. Once the morphology changes that occur during these "single cycle" experiments are understood then experiments will be performed to examine the morphological changes that occur during multicycle loading histories.

The multicycle experiments that are planned will involve changing the variables which may influence the behavior of the polyurethanes under cyclic deformation. These include varying the number of cycles, the initial and final deformation of a given cycle and the frequency of the deformation. It may be that the permanent deformation suffered by the hard segment domains in the polyurethane is more sensitive to some of these variables than others. These experiments should provide much needed insight into the morphological and mechanical behavior of polyurethanes subject to cyclic loading histories.

LIST OF FIGURES

## TABLE 1

| sample | molar ratio PTMO/MDI/BDO | mole fraction hard segment | weight % hard segment | average hard segment length[1] |
|---|---|---|---|---|
| 80A | 1/2.3/1.3 | 0.56 | 26 | 2.3 |
| 90A | 1/3.3/2.3 | 0.69 | 38 | 3.3 |
| 55D | 1/4.3/3.3 | 0.77 | 46 | 4.3 |

1 assuming random polymerization the number average hard segment length can be calculated from: $N = 1/(1-X)$ where X is the hard segment mole fraction.

## TABLE 2

| | $\epsilon_f$ (%) | $\sigma_f$ (N/m$^2$) x $10^{-7}$ |
|---|---|---|
| 80A | 600 | 6.34 |
| 90A | 500 | 5,65 |
| 55D | 480 | 6.41 |

## TABLE 3

| | $q_{max}$ (Å$^{-1}$) | d spacing (Å) |
|---|---|---|
| 80A | 0.056 | 110 |
| 90A | 0.069 | 90 |
| 55D | 0.069 | 90 |

## REFERENCES


1. I. Goodman, "Recent Developments in Block Copolymers", No. 2, Elsevier Applied Science Publishers, England, 1985

2. N.S. Schneider, C.R. Desper, J.L. Illinger, A.O. King and D Barr, J. Macromol. Sci.-Phys., 1975, **B11**, 527

3. A.L. Chang, R.M. Briber, P.E. Gibson, E.L. Thomas, R.J. Zdrahala, F.E. Critchfield, Polymer, 1982, **23**,1060

4. D.S. Huh and S.L. Cooper, Polym. Eng. Sci., 1971, **11**, 369

5. J. Blackwell and C.D. Lee, J. Polym. Sci., Polym. Phys. Ed., 1984, **22**, 759

6. T.R. Hesketh, J.W.C. Van Bogart, S.L. Cooper, Polym. Sci. and Eng.,1980, **20**, 190

7. G.L. Wilkes, S.L. Samuels, R. Crystal, J. Macromol. Sci.-Phys., 1974, **B10**, 203

8. R.W. Seymour, J.R. Overton, L.S. Corley, Macromolecules, 1975, **8**, 1975

9. R.M. Briber and E.L. Thomas, J. Polym. Sci., Polym. Phys. Ed., 1985, **23**, 1915

10. R.M. Briber and E.L. Thomas, J. Macromol. Sci.-Phys., 1984, **B22**, 509

11. R.M. Briber and P. Sung, Polym. Comm., 1987, **28(6)**, 162

12. Z. Ophir, G. Wilkes, J. Polym. Sci., Polym. Phys. Ed., 1980, **18**, 1469

13. J.T. Koberstein and R.S. Stein, J. Polym. Sci., Polym. Phys. Ed., 1983, **21**, 1483

14. J.W.C. Van Bogart, P.E. Gibson, S.L. Cooper, J. Polym. Sci., Polym. Phys. Ed., 1983, **21**, 65

15. C.R. Desper, N.S. Schneider, J.P. Jasinski, J.S. Lin, Macromolecules, 1985, **18**, 2755

16. M. Shibayama, Y. Ohki, T. Kotani, S. Nomura, Polym. Journ., 1987, **19(9)**, 1067

17. E.S. Kong, G.L. Wilkes, J. Polym. Sci., Polym. Lett. Ed., 1980, **18**, 369

18. R.W. Seymour, A.E. Allegreza, S.L. Cooper, Macromolecules, 1973, 6, 896

19. A.E. Allegreza, R.W. Seymour, H.N. Ng, S. L. Cooper, Polymer, 1974, **15**, 433

20. R. Bonart, J. Macrmol. Sci.-Phys., 1968, **B2(1)**, 115

21. Certain equipment, instruments or materials are identified in this paper in order to adequately specify the experimental details. Such identification does not imply recommendation by the National Institute of Standards and Technology or the Food and Drug Administration nor does it imply the materials or equipment identified are necessarily the best available for the purpose.

22. L.H. Peebles, Macromolecules, 1974, **7**, 872

23. L.H. Peebles, Macromolecules, 1976, **9**, 58

24. H.K. Frensdorff, Macromolecules, 1971, **4**, 369

25. R. Hosemann and S.N. Bagchi, "Direct Analysis of Diffraction by Matter", North Holland Publishing Company, Amsterdam, Interscience Publishers Inc., New York, 1962

26. R. Caspary, H. Schnecko, Makromol. Chem. 1981, **182**, 2109

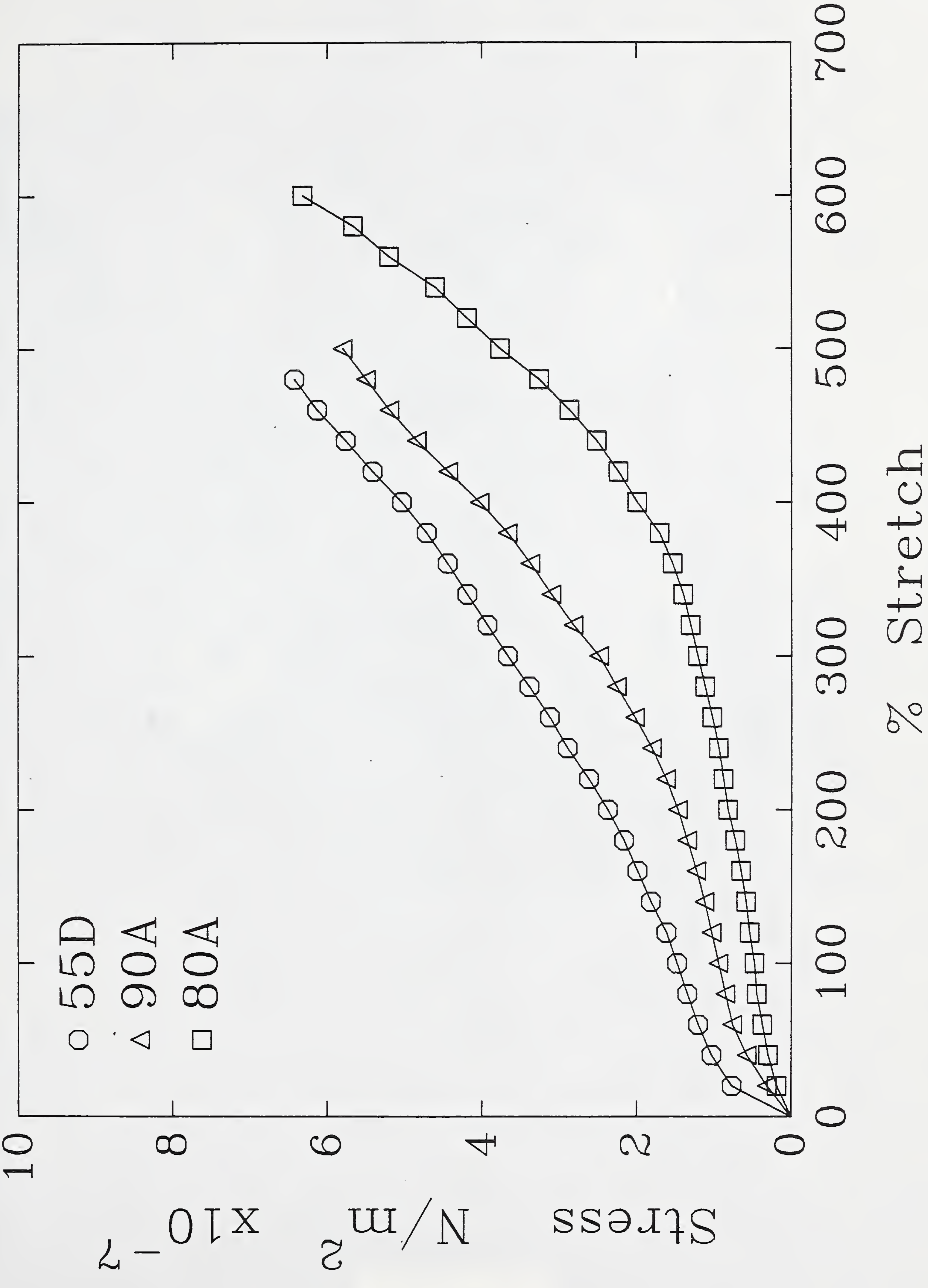

55D
90A
80A
Stress N/m2 x10-7
% Stretch
0
2
4
6
8
10
100
200
300
400
500
600
700


FIGURE 1

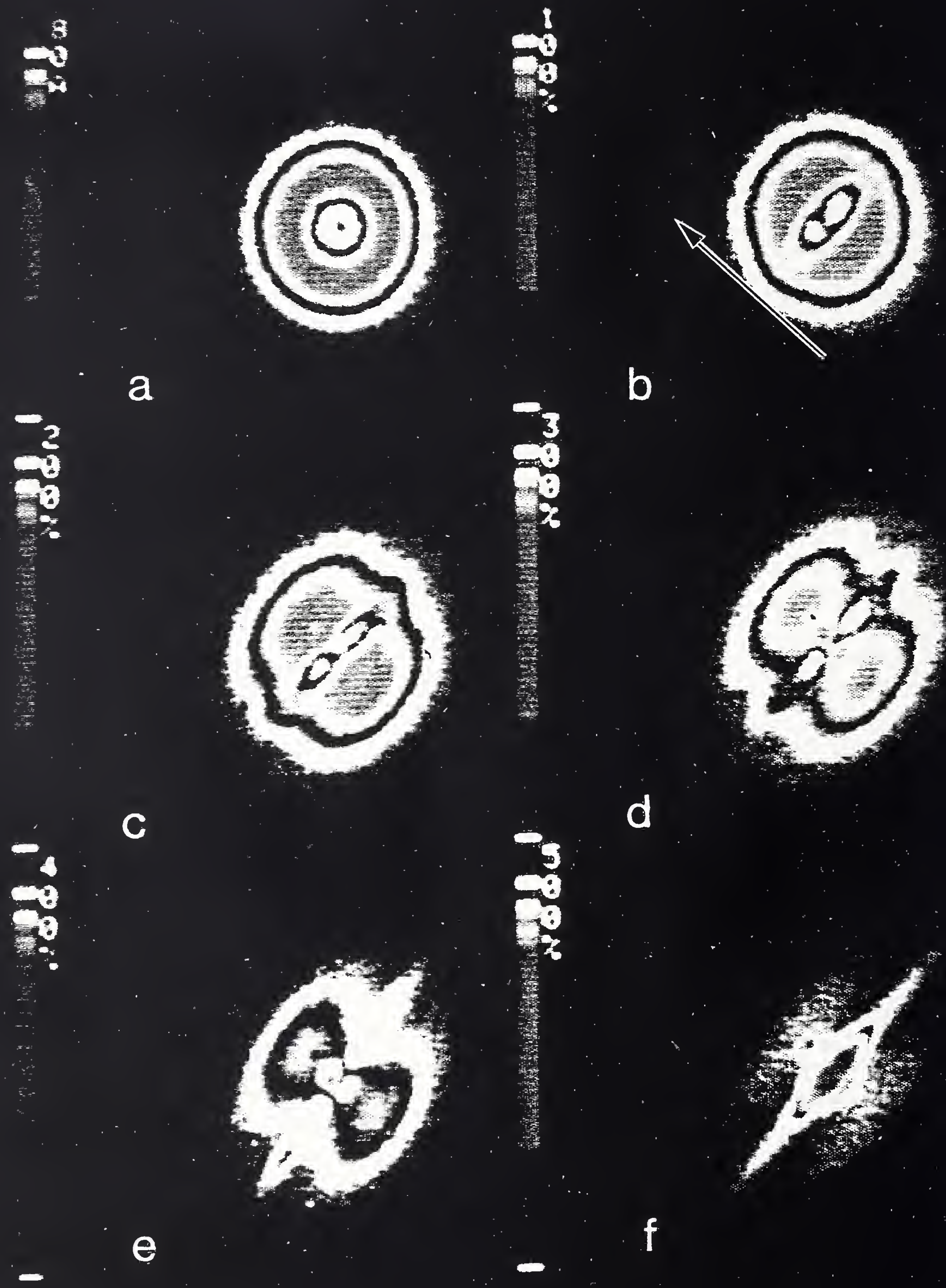


FIGURE 2


FIGURE 3

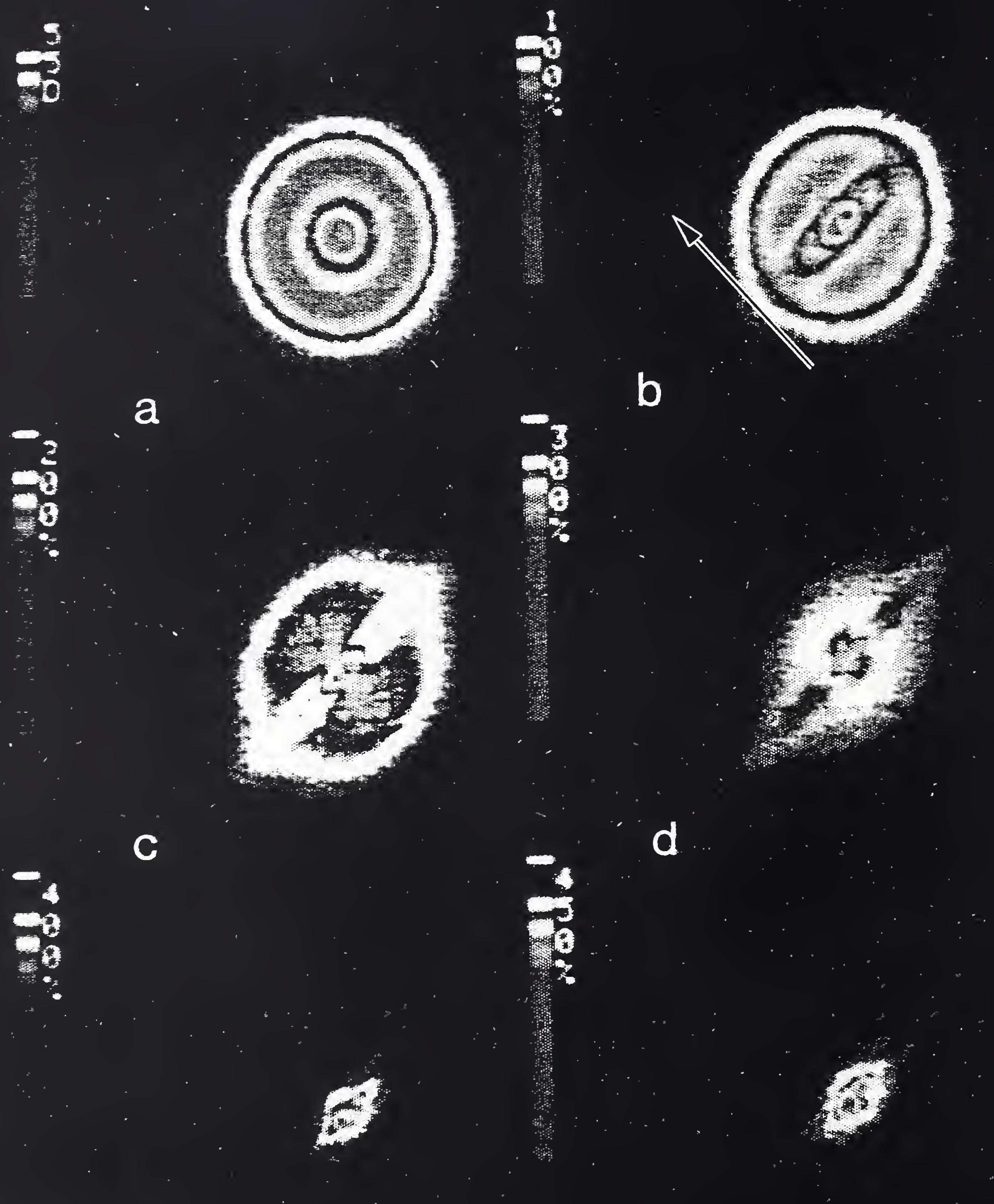


FIGURE 4

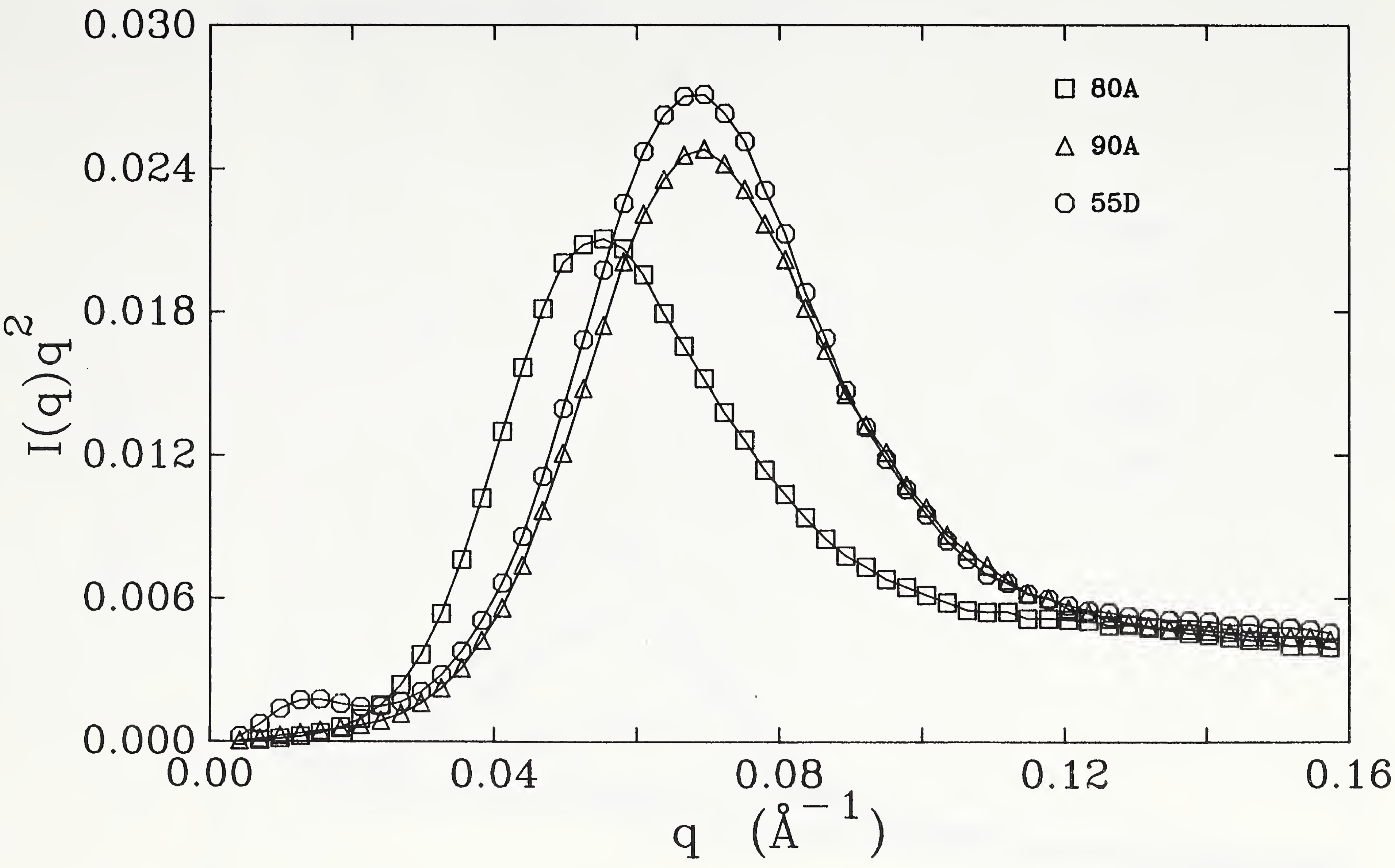
0.030
0.024
0.018
0.012
0.006
0.000
0.00
0.04
0.08
0.12
0.16
I(q)q2
q (Å-1)
80A
90A
55D

FIGURE 5

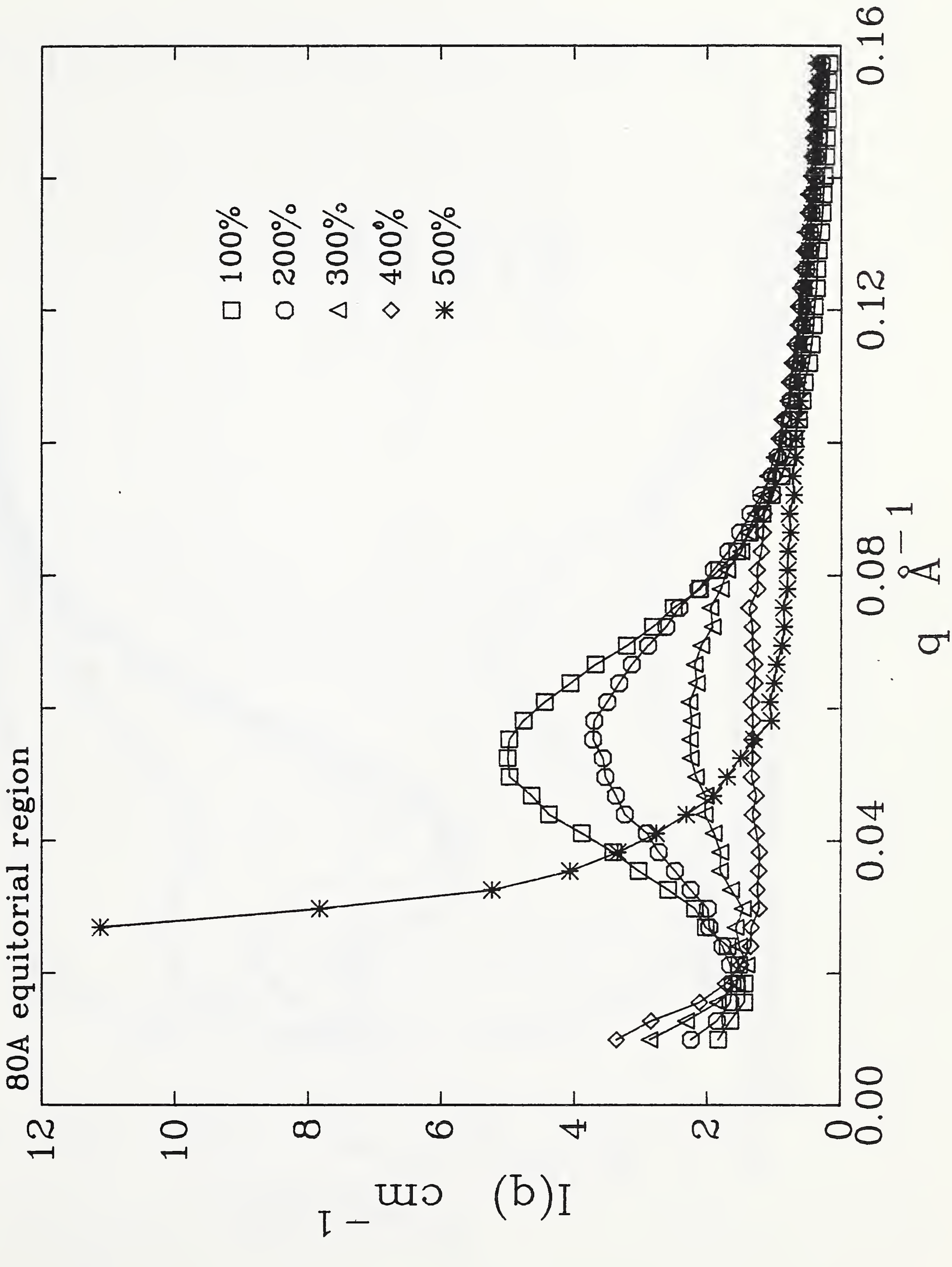

80A equitorial region
□ 100%
○ 200%
△ 300%
◇ 400%
✱ 500%
q Å$^{-1}$
I(q) cm$^{-1}$
0.00
0.04
0.08
0.12
0.16
0
2
4
6
8
10
12


FIGURE 6a

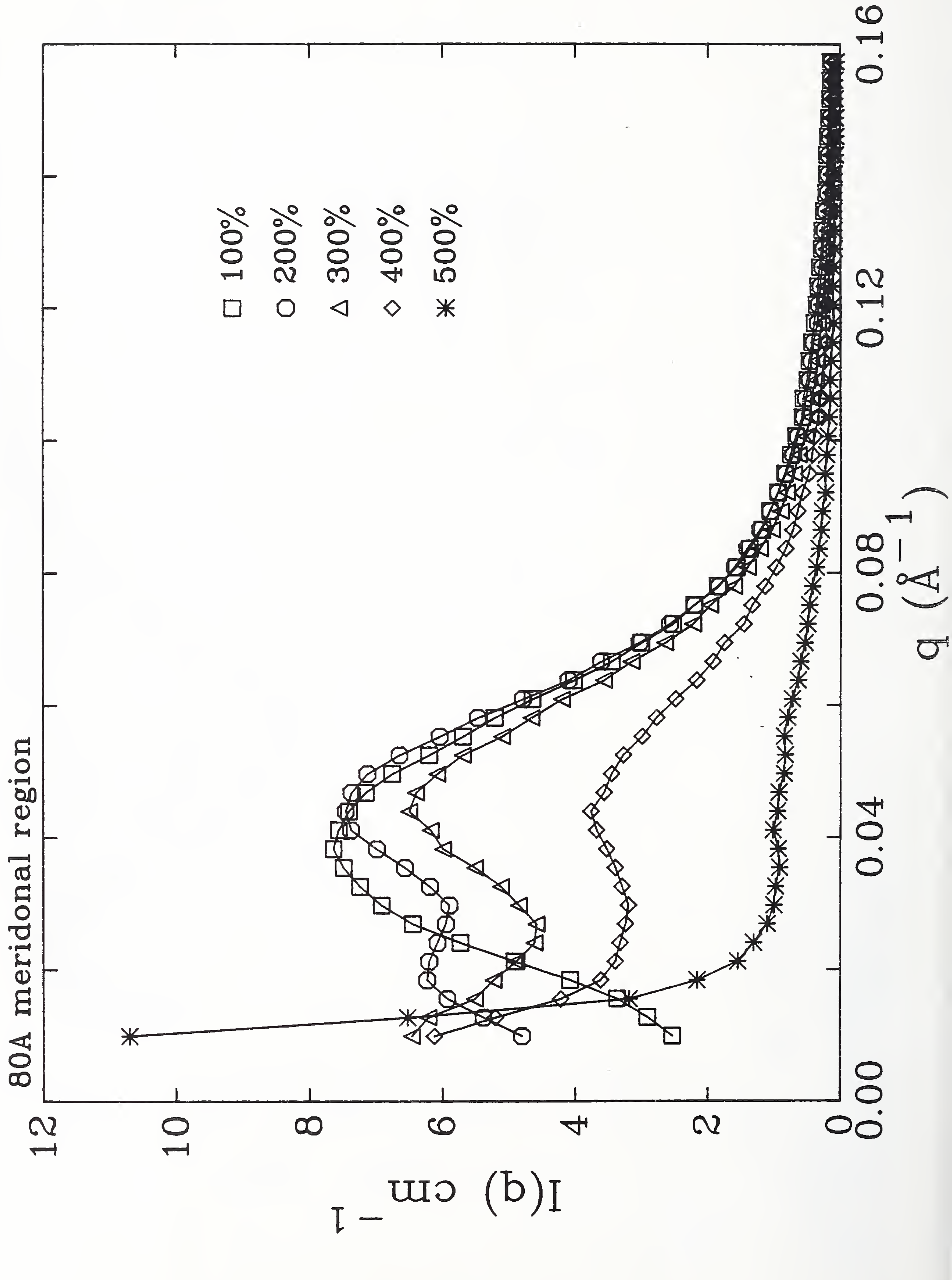

80A meridonal region
100%
200%
300%
400%
500%
I(q) cm$^{-1}$
q (Å$^{-1}$)
0
2
4
6
8
10
12
0.00
0.04
0.08
0.12
0.16


FIGURE 6b

b

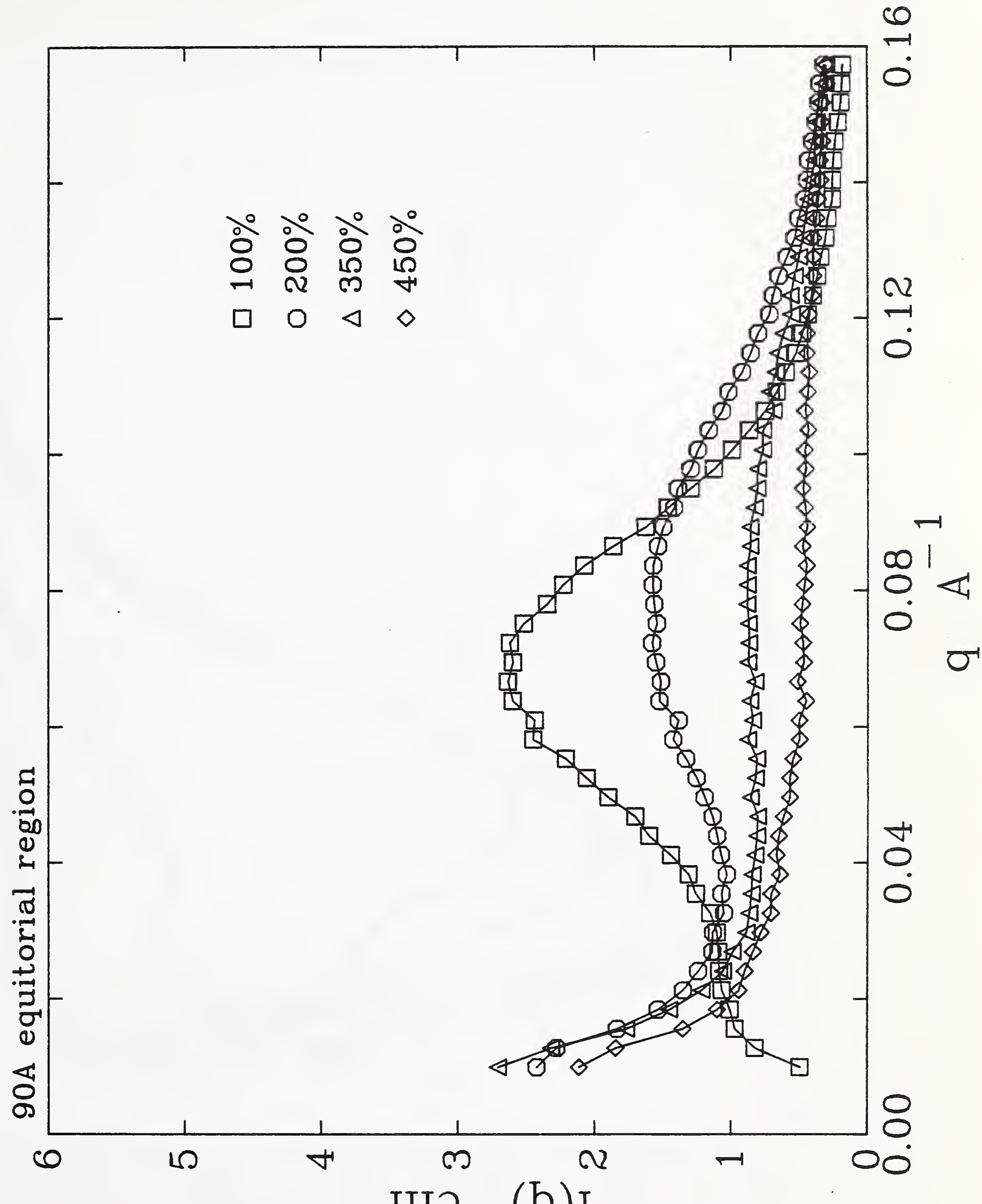
90A equitorial region
□ 100%
○ 200%
△ 350%
◇ 450%
I(q) cm$^{-1}$
q Å$^{-1}$
0
1
2
3
4
5
6
0.00
0.04
0.08
0.12
0.16

FIGURE 7a

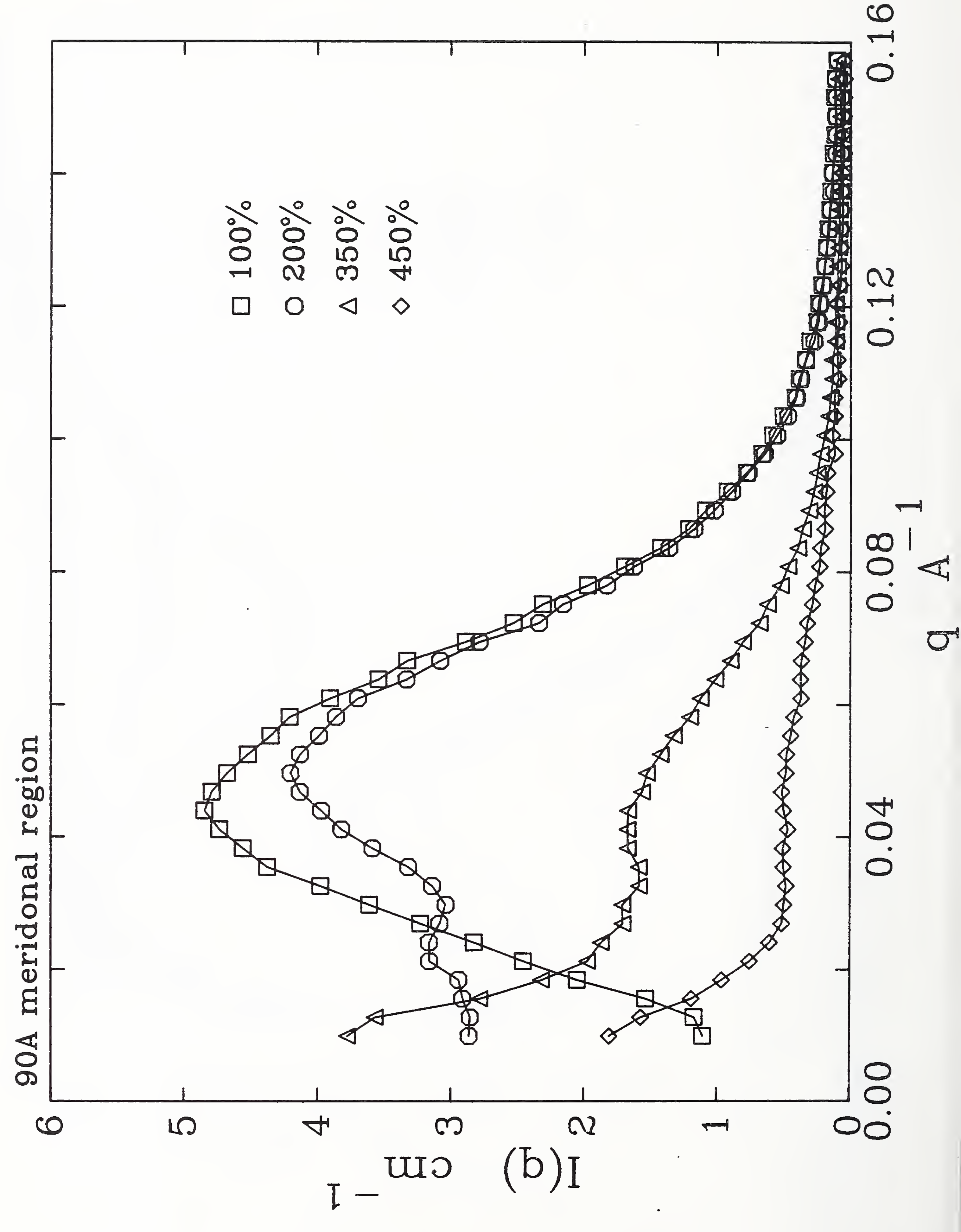

90A meridonal region
□ 100%
○ 200%
△ 350%
◇ 450%
I(q) cm$^{-1}$
q A$^{-1}$
0
1
2
3
4
5
6
0.00
0.04
0.08
0.12
0.16


FIGURE 7b

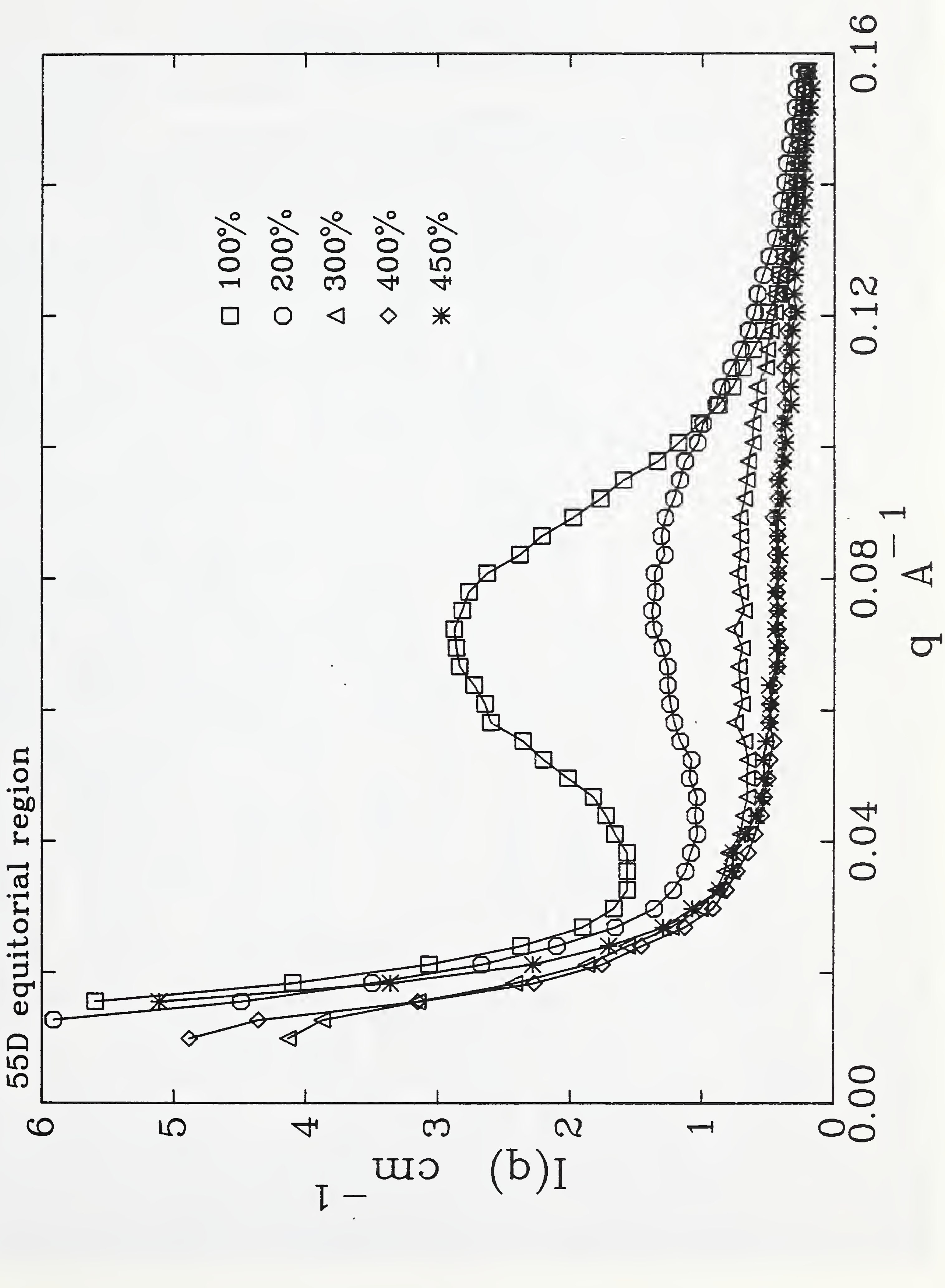
55D equitorial region
100%
200%
300%
400%
450%
I(q) cm^-1
q Å^-1
0.00
0.04
0.08
0.12
0.16
0
1
2
3
4
5
6

FIGURE 8a

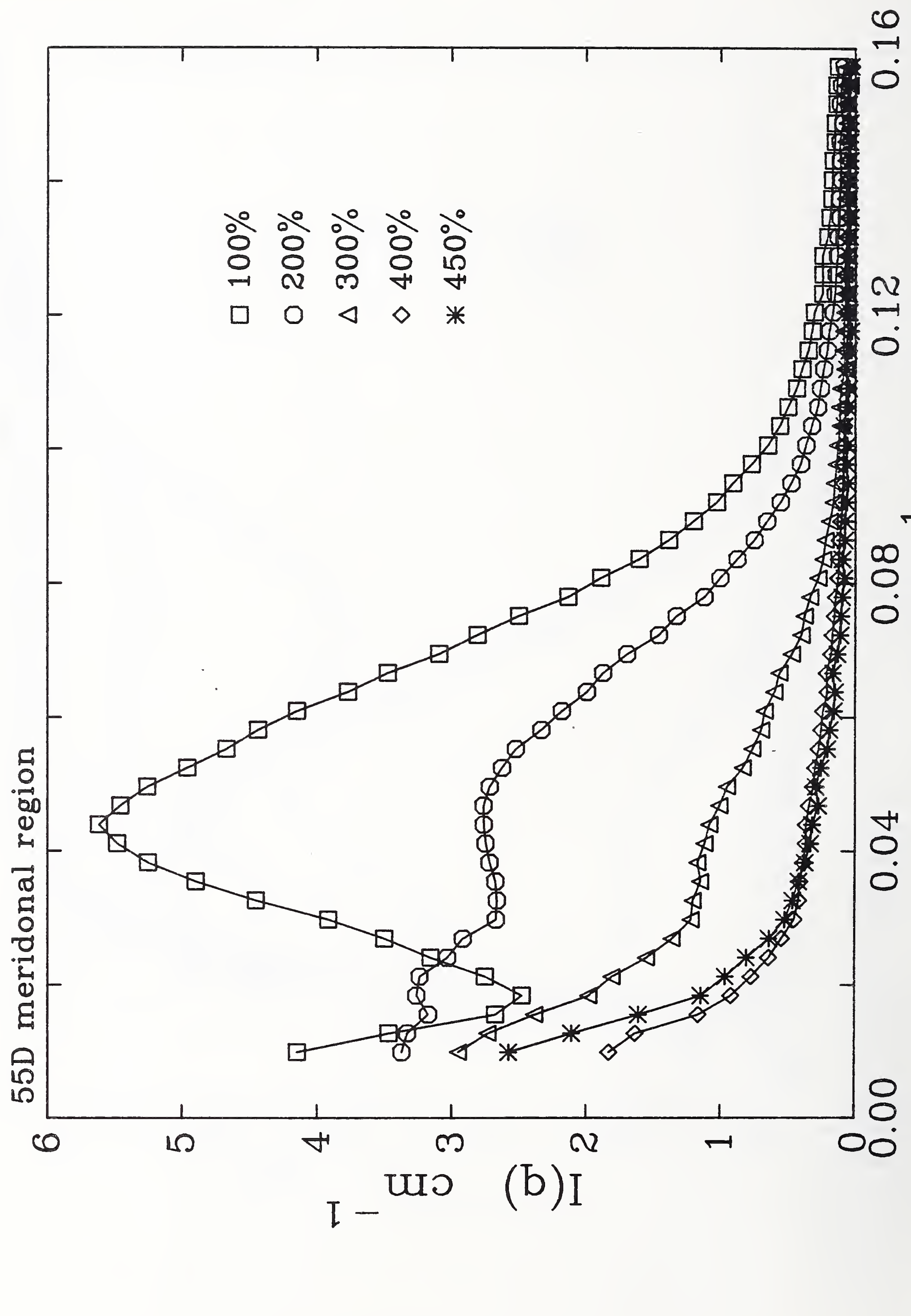
55D meridonal region
□ 100%
○ 200%
△ 300%
◇ 400%
✱ 450%
I(q) cm⁻¹
q Å⁻¹
0
1
2
3
4
5
6
0.00
0.04
0.08
0.12
0.16

FIGURE 8b

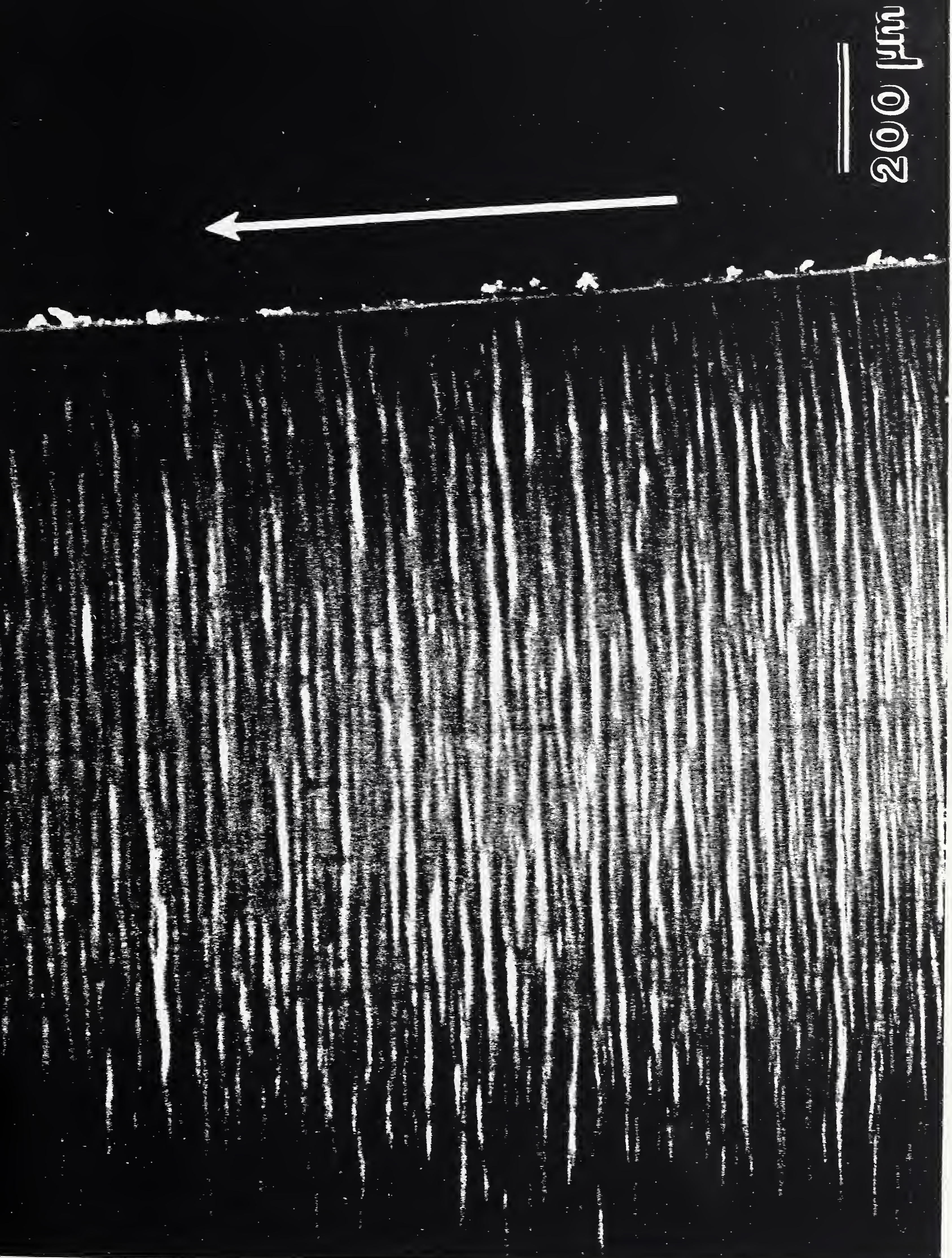


FIGURE 9a

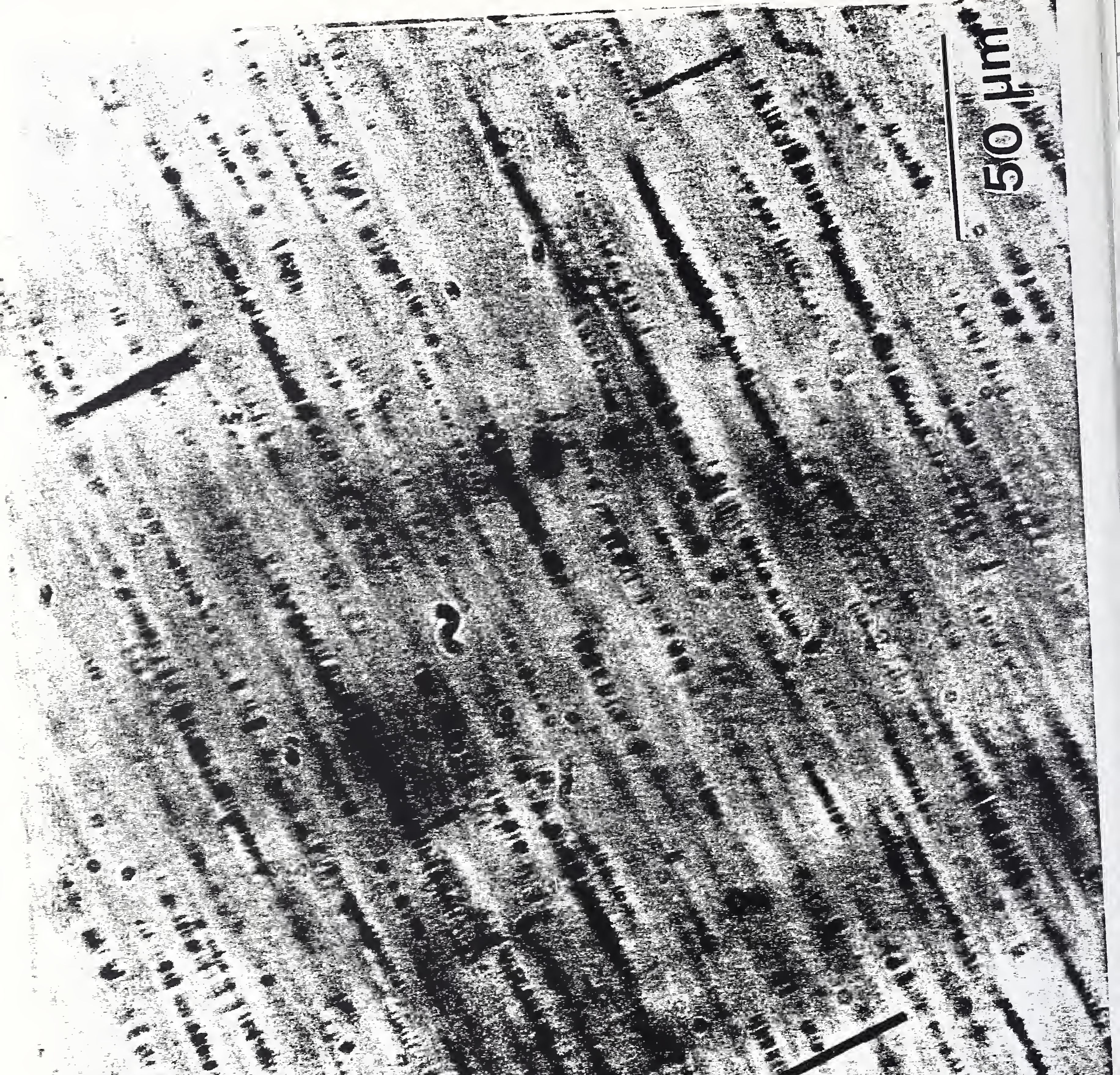


FIGURE 9b

NBS-114A (REV. 2-80)

| U.S. DEPT. OF COMM. BIBLIOGRAPHIC DATA SHEET (See instructions) | 1. PUBLICATION OR REPORT NO. NISTIR 88-3873 | 2. Performing Organ. Report No. | 3. Publication Date OCTOBER 1988 |
|---|---|---|---|

4. TITLE AND SUBTITLE

Small Angle X-Ray Scattering Study of the Deformation of MDI/BDO Based Polyurethanes

5. AUTHOR(S)

R. M. Briber; P. Sung, J. D. Barnes

6. PERFORMING ORGANIZATION (If joint or other than NBS, see instructions)

**NATIONAL BUREAU OF STANDARDS**
**U.S. DEPARTMENT OF COMMERCE**
**GAITHERSBURG, MD 20899**

7. Contract/Grant No.

8. Type of Report & Period Covered

9. SPONSORING ORGANIZATION NAME AND COMPLETE ADDRESS (Street, City, State, ZIP)

10. SUPPLEMENTARY NOTES

☐ Document describes a computer program; SF-185, FIPS Software Summary, is attached.

11. ABSTRACT (A 200-word or less factual summary of most significant information. If document includes a significant bibliography or literature survey, mention it here)

Small angle x-ray scattering (SAXS) has been used to study the effect of deformation on the hard segment domain morphology of a series of segmented polyurethanes based on MDI/BDO as the hard segment and PTMO as the soft segment. At relatively low elongations (100-200%) the hard segment lamellae orient and align with their long axis perpendicular to the deformation direction. As the deformation increases (200-400%) these aligned domains begin to break down and the SAX intensity decreases correspondingly. At the largest deformations (400-500%) a new component to the scattering appears as a streak running perpendicular to the deformation direction and subsequent optical microscopy revealed the presence of crazes. Crazes have been observed at elongations close to failure in all three polyurethanes studied so far, yet the presence of crazing has not been recognized in the scientific literature as being important in understanding the deformation behavior of polyurethanes.

12. KEY WORDS (Six to twelve entries; alphabetical order; capitalize only proper names; and separate key words by semicolons)

Polyurethanes, morphology, Small angle x-ray scattering, deformation, crazing

13. AVAILABILITY

☒ Unlimited
☐ For Official Distribution. Do Not Release to NTIS
☐ Order From Superintendent of Documents, U.S. Government Printing Office, Washington, D.C. 20402.
☒ Order From National Technical Information Service (NTIS), Springfield, VA. 22161

14. NO. OF PRINTED PAGES

29

15. Price

$11.95

USCOMM-DC 6043-P80